Geometry optimizations with the coupled-cluster model CC2 using the resolution-of-the-identity approximation

Christof Hättig[a)]
Forschungszentrum Karlsruhe, Institute of Nanotechnology, P.O. Box 3640, D-76021 Karlsruhe, Germany

(Received 30 July 2002; accepted 5 February 2003)

An implementation of the gradient for the second-order coupled-cluster singles-and-doubles model CC2 is reported, which employs the resolution-of-the-identity (RI) approximation for electron repulsion integrals. The performance of the CC2 model for ground state equilibrium geometries and harmonic frequencies is investigated and compared with experiment and other *ab initio* methods. It is found that CC2 equilibrium geometries have a similar accuracy to those calculated with second-order Møller–Plesset perturbation theory (MP2), but the bond lengths are larger. In particular, double and triple bonds and bonds in electron-rich compounds are elongated by 0.5–1.5 pm. Thereby CC2 slightly outperforms MP2 for single bonds, in particular in electron-rich compounds, but for strong double and triple bonds CC2 is somewhat inferior to MP2. The results for harmonic frequencies go in parallel with the results for equilibrium structures. The error introduced by the RI approximation is found to be negligible compared to the remaining one-electron basis set error, if optimized auxiliary basis sets are used. Typically, the RI error in bond lengths is of the order of 10^{-3} pm and the error in angles 10^{-3}–10^{-2} deg. Applications are reported for the geometry of *trans*-azobenzene and for the geometry and harmonic frequencies of *cis,trans*-1,4-difluorobutadiene. © *2003 American Institute of Physics.* [DOI: 10.1063/1.1564061]

I. INTRODUCTION

The determination of equilibrium geometries is one of the main issues of modern *ab initio* quantum chemistry and for a large variety of methods analytic gradients, which are required for efficient geometry optimizations, have been made available during the last decades. For well-behaved closed-shell molecules there exists also a well-established hierarchy of single-reference ''black box'' methods—density functional theory (DFT), second-order Møller–Plesset perturbation theory (MP2), coupled-cluster singles-and-doubles with a perturbative correction for connected triple-substitutions [CCSD(T)]—which at each level give significantly more accurate equilibrium geometries for, however, increased computational costs.[1] Also for a number of multi-reference methods analytic gradients are available today.

In the present communication an implementation of an analytic gradient for the second-order approximate coupled–cluster singles-and-doubles model CC2 is reported. The CC2 model was developed some years ago by Christiansen *et al.*[2] as an approximation to the CCSD method, which gives ground state energies and, for excited states dominated by single excitations, excitation energies correct through second order in the electron fluctuation potential. The computational costs for CC2 calculations scale as for MP2 with $\mathcal{O}(n^5)$, where n is a measure for the system size. However, the CC2 equations have to be solved iteratively which makes these calculations about an order of magnitude more expensive than MP2 calculations. Both methods give ground state energies correct through second order in the fluctuation potential and it is expected that MP2 and CC2 give results of similar accuracy; but different from the MP2 the CC2 model can also be applied for the calculation of excitation energies within the framework of response theory. For ground states, the main difference between MP2 and CC2 is that the latter model allows for a relaxation of connected single excitations, which are neglected in MP2, but this does not lead to a systematically improved accuracy. As will be shown in the following, this relaxation has, however, a notable effect on trends in the calculated equilibrium geometries.

From the above-presented discussion it is apparent that CC2 equilibrium geometries for electronic ground states will not be of much interest for themselves, since a similar accuracy is obtained with an order of magnitude smaller computational efforts if MP2 is used. The main application of the CC2 model is the calculation of excitation energies, where it is today—beside the configuration interaction singles with a perturbative correction for double-substitutions[3,4] [CIS(D)]—the only alternative to (TD)DFT[5] calculations, if the costly CCSD response cannot be applied. If only vertical excitation energies are needed, then such calculations can be done using any sufficiently accurate ground state geometry. If, however, adiabatic excitation energies are needed, then both the excited state and the ground state equilibrium geometries and the respective total energies should be determined by the same quantum chemical method. It will be these kinds of problems which will be the main application of a CC2 gradient.

Implementations of the ground state gradient for CC2 have been reported before by Christiansen *et al.*[6] and Halkier *et al.*[7–9] While the former was only a test implementation with an $\mathcal{O}(n^6)$ scaling of the operation count, the latter is an

[a)]Electronic mail: christof.haettig@int.fzk.de

 © 2003 American Institute of Physics

Downloaded 16 Apr 2003 to 141.52.232.84. Redistribution subject to AIP license or copyright, see http://ojps.aip.org/jcpo/jcpcr.jsp

integral-density direct implementation with an operation count scaling as $\mathcal{O}(ON^4)$, where N is the number of basis functions and O the number of occupied orbitals. The implementation reported here employs the resolution-of-the-identity (RI) approximation for the electron repulsion integrals (ERIs) in the correlation treatment. As described in a number of previous publications[10–13] the RI approximation leads for CC2 to a reduction of the operation count to $\mathcal{O}(O^2N^2N_x)$, where $N_x \approx 2-3N$ is the size of the auxiliary or fitting basis for the resolution of the identity. In practice, typically a reduction by about an order of magnitude or more is obtained.[10,13–15] The analytic gradient for the RI-CC2 approach will thus open the possibility for CC2 geometry optimizations for considerably larger molecules than has been possible with previous implementations. This is demonstrated in Sec. IV by applying the RI-CC2 gradient in calculations on the CC2 equilibrium geometry for the ground state of *trans*-azobenzene and the geometry and harmonic frequencies of *cis,trans*-1,4-difluorobutadiene.

Even though there have been two previous implementations[8,6] of the CC2 ground state gradient, only a few applications[6,16,17] have been reported and only little is known about the performance of the CC2 model for molecular structures. For this reason, the CC2 equilibrium geometries and harmonic frequencies are investigated in Sec. III for a number of small prototype molecules for which accurate experimental or *ab initio* reference data are available, and the accuracy and the trends of CC2 geometries are discussed. Particular focus is put on the comparison with the MP2 method and on the predictability of failures of CC2 by means of recently suggested diagnostics. The error introduced by the RI approximation compared to the result obtained with conventional four-index ERIs, the RI error, is demonstrated to be insignificant; typically of the order 10^{-3} pm for bond lengths and $10^{-3}-10^{-2}$ deg for angles.

II. ANALYTIC FIRST DERIVATIVES FOR THE CC2 MODEL

The Lagrange function for the (orbital-relaxed) CC2 model is

$$\begin{aligned} L^{\mathrm{CC2}} &= \langle \mathrm{HF}|\hat{H}+[\hat{H},T_2]|\mathrm{HF}\rangle \\ &+ \sum_{\mu_2} \overline{t}_{\mu_2}\langle \mu_2|\hat{H}+[F,T_2]|\mathrm{HF}\rangle \\ &+ \sum_{\mu_1} \overline{t}_{\mu_1}\langle \mu_1|\hat{H}+[\hat{H},T_2]|\mathrm{HF}\rangle + \sum_{\mu_0} \overline{\kappa}_{\mu_0}F_{\mu_0}, \end{aligned} \tag{1}$$

where $\overline{t}_{\mu_1}, \overline{t}_{\mu_2}$ are the Lagrangian multipliers for, respectively, the singles and the doubles part of the cluster equations and $\overline{\kappa}_{\mu_0}$ the Lagrangian multipliers for the orbital rotations. The Hartree–Fock (HF) determinant is thereby parametrized as

$$|\mathrm{HF}\rangle = \exp\left(\sum_{\mu_0} \kappa_{\mu_0}(E_{\mu_0}-E_{\mu_0}^{\dagger})\right)|\mathrm{HF}_0\rangle, \tag{2}$$

where $|\mathrm{HF}_0\rangle$ is a suitable reference determinant chosen such that for the unperturbed system $\kappa_{\mu_0}=0$. The cluster operator is written as $T=\Sigma_{i=1}^{2} T_i$ with $T_i=\Sigma_{\mu_i} t_{\mu_i}\tau_{\mu_i}$. For a closed shell reference state we choose $\tau_{ai}=E_{ai}$ and $\tau_{aibj}=E_{ai}E_{bj}$, where i, j denote active occupied and a, b active virtual orbitals. The operators E_{pq} are the usual second quantization singlet excitation operators.[1] For convenience, we introduced in Eq. (1) the similarity transformed Hamiltonian:

$$\hat{H}=e^{-T_1}He^{T_1}=\sum_{pq} \hat{h}_{pq}E_{pq}+\frac{1}{2}\sum_{pqrs} (pq\hat{|}rs)e_{pqrs}. \tag{3}$$

Here and in the following, indices p,q,r,s denote any occupied or virtual molecular orbital. If the CC2 model is used in conjunction with the RI approximation, all electron repulsion integrals entering in the correlation treatment are approximated by an expansion in an auxiliary basis,[18–21]

$$(pq|rs)^{\mathrm{RI}}=\sum_{PQ} (pq|P)V_{PQ}^{-1}(Q|rs), \tag{4}$$

$$V_{PQ}=(P|Q), \tag{5}$$

while the Hartree–Fock contribution to the total energy and the self-consistent field (SCF) Fock operator,

$$F_{pq}=h_{pq}+\sum_{rs} D_{rs}^{\mathrm{SCF}}\left[(pq|rs)-\frac{1}{2}(ps|rq)\right], \tag{6}$$

are evaluated in a preceding SCF calculation, which is carried out with conventional four-index ERIs. To distinguish carefully between contributions and intermediates calculated from conventional ERIs and those evaluated using the RI approximation, we write the Lagrangian as

$$\begin{aligned} L^{\mathrm{RI\text{-}CC2}} &= \langle \mathrm{HF}|H|\mathrm{HF}\rangle + \sum_{pq} D_{pq}^{F}F_{pq} + \sum_{\mu_0} \overline{\kappa}_{\mu_0}F_{\mu_0} \\ &+ \frac{1}{2}\sum_{pqrs} d_{pqrs}^{\Lambda,\mathrm{nsep}}(pq\hat{|}rs)^{\mathrm{RI}} \end{aligned} \tag{7}$$

with

$$\begin{aligned} D_{pq}^{F} &= \langle \mathrm{HF}|[E_{pq},T_1]|\mathrm{HF}\rangle \\ &+ \sum_{\mu_1} \overline{t}_{\mu_1}\langle \mu_1|e^{-T_1}E_{pq}e^{T_1}+[E_{pq},T_2]|\mathrm{HF}\rangle \\ &+ \sum_{\mu_2} \overline{t}_{\mu_2}\langle \mu_2|[E_{pq},T_2]|\mathrm{HF}\rangle, \end{aligned} \tag{8}$$

$$\begin{aligned} d_{pqrs}^{\Lambda,\mathrm{nsep}} &= \langle \mathrm{HF}|[[e_{pqrs},T_1],T_1]+[e_{pqrs},T_2]|\mathrm{HF}\rangle \\ &+ \sum_{\mu_1} \overline{t}_{\mu_1}\langle \mu_1|[e_{pqrs},T_1]+[e_{pqrs},T_2]|\mathrm{HF}\rangle \\ &+ \sum_{\mu_2} \overline{t}_{\mu_2}\langle \mu_2|e_{pqrs}|\mathrm{HF}\rangle, \end{aligned} \tag{9}$$

where the integrals $(pq\hat{|}rs)^{\mathrm{RI}}$ refer to the basis of the similarity transformed Hamiltonian $\hat{H}$, denoted as Λ^p,Λ^h basis. For the respective two-particle density therefore a superscript Λ is used; nsep indicates that this is the nonseparable correlation contribution to the two-particle density (*vide infra*). Explicit expressions for the matrices D^F and $d^{\Lambda,\mathrm{nsep}}$ are given in Table I. Both densities have nonvanishing elements

Downloaded 16 Apr 2003 to 141.52.232.84. Redistribution subject to AIP license or copyright, see http://ojps.aip.org/jcpo/jcpcr.jsp

TABLE I. The density matrices D^F and $d^{\Lambda,\mathrm{nsep}}$. For the density $d^{\Lambda,\mathrm{nsep}}$ only the unique nonvanishing blocks are listed; the other nonvanishing blocks $d^{\Lambda,\mathrm{nsep}}_{kaij}$, $d^{\Lambda,\mathrm{nsep}}_{abij}$, $d^{\Lambda,\mathrm{nsep}}_{bcia}$, and $d^{\Lambda,\mathrm{nsep}}_{aijb}$ are related to the given blocks by the particle exchange symmetry $d^{\Lambda}_{pqrs}=d^{\Lambda}_{rspq}$. Indices i,j,k refer to active occupied and indices a,b,c to active virtual molecular orbitals. Note, that there are no frozen-core contributions to D^F and $d^{\Lambda,\mathrm{nsep}}$. For the definition of C_{ai} see Table II.

$$
\begin{aligned}
&D^F_{ij}=-\Sigma_{abk}\bar{t}^{ab}_{jk}t^{ab}_{ik}-\Sigma_a\bar{t}_{aj}t_{ai}\\
&D^F_{ia}=C_{ai}+2t_{ai}-\Sigma_{bj}\bar{t}_{bj}t_{bi}t_{aj}\\
&D^F_{ai}=\bar{t}_{ai}\\
&D^F_{ab}=\Sigma_{ijc}\bar{t}^{ac}_{ij}t^{bc}_{ij}+\Sigma_i\bar{t}_{ai}t_{bi}\\
&d^{\Lambda,\mathrm{nsep}}_{ijka}=-\Sigma_b\bar{t}_{bj}[2t^{ba}_{ik}-t^{ba}_{ki}]\\
&d^{\Lambda,\mathrm{nsep}}_{ijab}=-\bar{t}_{aj}t_{bi}\\
&d^{\Lambda,\mathrm{nsep}}_{iajb}=2(2-\hat{P}_{ij})(t^{ab}_{ij}+t_{ai}t_{bj}+C_{ai}t_{bj})\\
&d^{\Lambda,\mathrm{nsep}}_{iabj}=2\bar{t}_{bj}t_{ai}\\
&d^{\Lambda,\mathrm{nsep}}_{iabc}=\Sigma_j t_{bj}[2t^{ca}_{ji}-t^{ca}_{ij}]\\
&d^{\Lambda,\mathrm{nsep}}_{aibj}=\bar{t}^{ab}_{ij}
\end{aligned}
$$

only in the active occupied and virtual spaces. Note, that with this formulation there are no frozen-core contributions to the density matrices D^F and d^{Λ}. The frozen-core contributions, coming from the Hartree–Fock contribution to the energy and the contributions from the SCF Fock matrix F, enter only via the SCF one-particle density and the separable part of the two-particle density (*vide infra*), which makes the implementation of the frozen-core approximation for the gradient an easy task.

As usual, the equations for both the Lagrangian multipliers $\bar{t}_\mu$ and $\bar{\kappa}_{\mu_0}$ and the wave function parameters t_μ and κ_{μ_0} are obtained by requiring L^{CC2} to be stationary in its variables. The equations for t_μ and $\bar{t}_\mu$ and their implementation within the RI-CC2 approach have been reported in preceding communications[10,12,13] and will not be discussed here further. The orbital rotation parameters κ_{μ_0} vanish for the unperturbed system due to the parametrization chosen in Eq. (2). The index range of κ_{μ_0} and the corresponding Lagrangian multipliers $\bar{\kappa}_{\mu_0}$ depend on the constraints applied to the SCF Fock operator, i.e., whether a canonical or a noncanonical[22] or semicanonical[23–25] representation is chosen. In any case, the occupied/virtual block $\bar{\kappa}_{IA}$ is obtained as solution of the CPHF equations also known as Z-vector equations:

$$
\sum_{AIBJ}\bar{\kappa}_{AI}(A_{AIBJ}+\delta_{AB}\epsilon_A-\delta_{IJ}\epsilon_I)=-\eta^{\kappa}_{BJ}=-\frac{\partial L^{\mathrm{CC2}}}{\partial\kappa_{BJ}}, \tag{10}
$$

where the indices I,J and A,B denote, respectively, general (i.e., active and frozen) occupied and virtual indices and ϵ_p the SCF orbital energies. The matrix A_{pqrs} is defined as $A_{pqrs}=4(pq|rs)-(pr|sq)-(ps|rq)$ with conventional four-index ERIs.

Analytic first derivatives with respect to an external parameter x, as, e.g., the gradient, can then be calculated as

$$
\begin{aligned}
\frac{dL^{\mathrm{CC2}}}{dx}&=\frac{\partial L^{\mathrm{CC2}}}{\partial x}\\
&=\sum_{\alpha\beta}D^{\mathrm{eff,ao}}_{\alpha\beta}h^{[x]}_{\alpha\beta}+\frac{1}{2}\sum_{\alpha\beta\gamma\delta}d^{\mathrm{sep,ao}}_{\alpha\beta\gamma\delta}(\alpha\beta|\gamma\delta)^{[x]}\\
&\quad-\sum_{\alpha\beta}F^{\mathrm{eff,ao}}_{\alpha\beta}S^{[1]}_{\alpha\beta}+\sum_{\alpha\beta P}\Delta^{\mathrm{ao},P}_{\alpha\beta}(\alpha\beta|P)^{[x]}\\
&\quad-\sum_{PQ}\gamma_{PQ}V^{[x]}_{PQ}.
\end{aligned}
\tag{11}
$$

In Eq. (11) the indices $\alpha,\beta,\gamma,\delta$ refer to the atomic orbital basis and the superscript $[x]$ indicates first derivatives with respect to the parameter x. The relaxed one-particle density $D^{\mathrm{eff,ao}}$ and the separable part of the two-particle density $d^{\mathrm{sep,ao}}$, which has to be contracted with derivatives of four-index integrals, are obtained as

$$
D^{\mathrm{eff,ao}}_{\alpha\beta}=\sum_{pq}C_{\alpha p}C_{\beta q}D^{\mathrm{eff}}_{pq}, \tag{12}
$$

$$
D^{\mathrm{eff,ao}}_{pq}=D^{\mathrm{SCF}}_{pq}+D^F_{pq}+(\bar{\kappa}_{pq}+\bar{\kappa}_{qp})/2, \tag{13}
$$

$$
d^{\mathrm{sep,ao}}_{\alpha\beta\gamma\delta}=\hat{P}^{\alpha\gamma}_{\beta\delta}\left(1-\frac{1}{2}\hat{P}_{\beta\delta}\right)\left(D^{\mathrm{eff,ao}}_{\alpha\beta}-\frac{1}{2}D^{\mathrm{SCF,ao}}_{\alpha\beta}\right)D^{\mathrm{SCF,ao}}_{\gamma\delta}, \tag{14}
$$

where $\hat{P}_{\beta\delta}$ is an operator which permutes the two indices β and δ. Due to its simple structure $d^{\mathrm{sep,ao}}$ can be constructed on-the-fly from $D^{\mathrm{eff,ao}}_{\alpha\beta}$ and $D^{\mathrm{SCF,ao}}_{\alpha\beta}$ and contracted with the integrals $(\alpha\beta|\gamma\delta)^{[x]}$ without storing any four-index intermediates in memory or on disk or employing multipass algorithms.

The three- and two-index two-particle densities $\Delta^{\mathrm{ao},P}$ and γ_{PQ} are defined as

$$
\Delta^{\mathrm{ao},P}_{\alpha\beta}=\sum_{pq}\Lambda^p_{\alpha p}\Lambda^h_{\beta q}\sum_{rsQ}d^{\Lambda,\mathrm{nsep}}_{pqrs}(rs\hat{|}Q)V^{-1}_{QP}, \tag{15}
$$

$$
\gamma_{PQ}=\sum_{\alpha\beta R}\Delta^{\mathrm{ao},P}_{\alpha\beta}(\alpha\beta|R)V^{-1}_{RQ}, \tag{16}
$$

where $\Lambda^P=\mathbf{C}(\mathbf{1}-\mathbf{t}_1^T)$ and $\Lambda^h=\mathbf{C}(\mathbf{1}+\mathbf{t_1})$ are the ao-to-MO transformation matrices for the similarity transformed basis introduced in Eq. (3).

The intermediate $F^{\mathrm{eff,ao}}$ is the usual effective Fock matrix used to formulate derivatives of correlated methods,[26] also known as energy weighted density matrix, which is here adapted for the RI-CC2 approach and written in the contravariant ao basis:

$$
\begin{aligned}
F^{\mathrm{eff,ao}}_{\alpha\beta}&=\sum_{pq}C_{\alpha p}C_{\beta q}\frac{1}{2}(D^{\mathrm{eff}}_{pq}+D^{\mathrm{eff}}_{qp})\epsilon_q\\
&\quad+\sum_{Ip}C_{\alpha I}C_{\beta q}\sum_{rs}(D^F_{rs}+\bar{\kappa}_{rs})A_{rsIq}\\
&\quad+\sum_{pq}C_{\alpha p}C_{\beta q}\sum_{rst}\frac{1}{2}(d^{\mathrm{nsep}}_{rstp}+d^{\mathrm{nsep}}_{rspt})(rs|tq)^{\mathrm{RI}},
\end{aligned}
\tag{17}
$$

Downloaded 16 Apr 2003 to 141.52.232.84. Redistribution subject to AIP license or copyright, see http://ojps.aip.org/jcpo/jcpcr.jsp

TABLE II. Intermediates used to calculate the three-index two-particle density matrix $\Delta^{\mathrm{ao},Q}_{\alpha\beta}$, the effective Fock matrix $F^{\mathrm{eff,ao}}_{\alpha\beta}$ and the inhomogeneity η^{κ}_{AI}.

$$\Gamma^{(a),Q}_{j\beta}=\Sigma_p C_{\beta p}\Sigma_P V^{-1/2}_{PQ}\tilde{Y}^P_{pj}$$
$$\Gamma^{(b),Q}_{j\beta}=\Sigma_a \Lambda^p_{\beta a}\Sigma_P V^{-1/2}_{PQ}\check{Y}^P_{aj}$$
$$\Gamma^{(c),Q}_{j\beta}=\Sigma_p C_{\beta p}\Sigma_P V^{-1/2}_{PQ}Y^{\star P}_{pj}$$
$$\tilde{Y}^P_{pj}=\Sigma_a(Y^P_{aj}+\Sigma_c\hat{B}^P_{ac}t_{cj})\check{\lambda}^h_{pa}+\Sigma_a\Delta^P_{ja}\lambda^h_{pa}$$
$$\Delta^P_{jb}=Y^P_{bj}+\bar{Y}^P_{bj}+2t_{bj}\Sigma_k S^P_{kk}-\Sigma_k t_{bk}S^P_{kj}$$
$$+2C_{bj}\Sigma_k\hat{I}^P_{kk}-\Sigma_k C_{bk}\hat{I}^P_{jk}+2t_{bj}\Sigma_{ck}\bar{t}_{ck}\hat{B}^P_{ck}$$
$$Y^{\star,P}_{pi}=\Sigma_b(Y^P_{bi}-\Sigma_k t_{bk}\hat{B}^P_{ki})\lambda^h_{pb}+2\lambda^h_{pi}\Sigma_k\hat{I}^P_{kk}$$
$$Y^P_{ai}=\Sigma_{bj}(2t^{ab}_{ij}-t^{ab}_{ji})\hat{B}^P_{bj}$$
$$\bar{Y}^P_{ai}=\Sigma_{bj}(2t^{ab}_{ij}-t^{ab}_{ji})\bar{B}^P_{bj}$$
$$\check{Y}^P_{ai}=\Sigma_{bj}\bar{t}^{ab}_{ij}\hat{B}^P_{bj}$$
$$B^P_{pq}=\Sigma_{\alpha\beta Q}C_{\alpha p}C_{\beta q}(\alpha\beta|Q)V^{-1/2}_{PQ}$$
$$\hat{B}^P_{pq}=\Sigma_{\alpha\beta Q}\Lambda^p_{\alpha p}\Lambda^h_{\beta q}(\alpha\beta|Q)V^{-1/2}_{PQ}$$
$$\check{B}^P_{pq}=\Sigma_{\alpha\beta Q}(\check{\Lambda}^p_{\alpha p}\Lambda^h_{\beta q}+\Lambda^p_{\alpha p}\check{\Lambda}^h_{\beta q})(\alpha\beta|Q)V^{-1/2}_{PQ}$$
$$\hat{I}^P_{ij}=\Sigma_c\hat{B}^P_{ic}t_{cj}$$
$$S^P_{ij}=\hat{I}^P_{ij}+\Sigma_c\hat{B}^P_{ic}C_{cj}$$
$$C_{ai}=\Sigma_{bj}(2t^{ab}_{ij}-t^{ab}_{ji})\bar{t}_{bj}$$
$$\check{\Lambda}^p=C\check{\lambda}^p \qquad \check{\lambda}^p=(1-t_1{}^T)\bar{t}$$
$$\check{\Lambda}^h=C\check{\lambda}^h \qquad \check{\lambda}^h=(1+t_1)\bar{t}^T$$

Related to F^{eff} is the right-hand-side vector for the Z-vector equations, which is given by

$$\eta^{\kappa}_{AI}=\frac{1}{2}(D^F_{AI}+D^F_{IA})(\epsilon_I-\epsilon_A)-\frac{1}{4}\sum_{pq}(D^F_{pq}+D^F_{qp})A_{pqAI}$$
$$+\sum_{pqrs}[(d^{\mathrm{nsep}}_{pArs}+d^{\mathrm{nsep}}_{Aprs})(pI|rs)^{\mathrm{RI}}$$
$$-(d^{\mathrm{nsep}}_{pIrs}+d^{\mathrm{nsep}}_{Iprs})(Ap|rs)^{\mathrm{RI}}]. \tag{18}$$

In Eqs. (17) and (18) we used for convenience the two-particle density in the canonical MO basis $d^{\mathrm{nsep}}_{pqrs}=\Sigma_{p'q'r's'}\lambda^p_{pp'}\lambda^h_{qq'}\lambda^p_{rr'}\lambda^h_{ss'}d^{\Lambda,\mathrm{RI}}_{p'q'r's'}$ with the transformation matrices $\lambda^P=\mathbf{1}-\mathbf{t}_1^T$ and $\lambda^h=\mathbf{1}+\mathbf{t}_1$.

The most important intermediate for the calculation of the RI-CC2 gradient is the three-index density $\Delta^{\mathrm{ao},P}_{\alpha\beta}$. Storage of $\Delta^{\mathrm{ao},P}_{\alpha\beta}$ either in memory or on disk would require $\mathcal{O}(N^2N_x)$ words, where N is the number of basis functions and $N_x\approx 2.5N$ the size of the auxiliary basis set. For large scale calculations this would lead to a storage bottleneck. Therefore $\Delta^{\mathrm{ao},P}$ is rewritten in terms of three smaller intermediates $\Gamma^{(a)}$, $\Gamma^{(b)}$, and $\Gamma^{(c)}$, which can more easily be stored on disk, and three transformation matrices:

$$\Delta^{\mathrm{ao},Q}_{\alpha\beta}=\sum_j\{C_{\alpha j}\Gamma^{(a),Q}_{j\beta}+\Gamma^{(b),Q}_{j\alpha}\Lambda^h_{\beta j}+\check{\Lambda}^p_{\alpha j}\Gamma^{(c),Q}_{j\beta}\}. \tag{19}$$

Explicit expressions for these intermediates and the transformation matrices are given in Table II. The same intermediates can be used to calculate the contribution of $\Delta^{\mathrm{ao},P}$ to $F^{\mathrm{eff,ao}}$ and to the right-hand-side vector for the Z-vector equations η^{κ}_{AI}. For this we introduce for each Γ intermediate two matrices H_{pq} and Ω_{pq} for which the expressions are given Table III. With these matrices $F^{\mathrm{eff,ao}}$ and η^{κ} can be calculated as

TABLE III. Definition matrices H and Ω. The matrices are defined here for general (i.e., frozen and active) indices, but their elements are nonzero only if p refers to an active orbital, while q may also refer to frozen occupied or virtual orbital.

$$H^{(a)}_{pq}=\Sigma_{Qi}\tilde{Y}_{pi}B^Q_{iq}$$
$$H^{(b)}_{pq}=\Sigma_a\lambda^p_{pa}\Sigma_{Qi}\check{Y}_{ai}\Sigma_r\lambda^h_{rj}B^Q_{qr}$$
$$H^{(c)}_{pq}=\Sigma_{Qi}Y^{\star,Q}_{pj}\Sigma_r\lambda^p_{rj}B^Q_{rq}$$
$$\Omega^{(a)}_{qp}=\Sigma_\alpha C_{\alpha q}\Sigma_j\lambda^p_{pj}\Sigma_{Q\beta}\Gamma^{(a),Q}_{j\beta}(\alpha\beta|Q)$$
$$\Omega^{(b)}_{qp}=\Sigma_\alpha C_{\alpha q}\Sigma_j\lambda^h_{pj}\Sigma_{Q\beta}\Gamma^{(b),Q}_{j\beta}(\alpha\beta|Q)$$
$$\Omega^{(c)}_{qp}=\Sigma_\alpha C_{\alpha q}\Sigma_j\check{\lambda}^p_{pj}\Sigma_{Q\beta}\Gamma^{(c),Q}_{j\beta}(\alpha\beta|Q)$$

$$F^{\mathrm{eff,ao}}_{\alpha\beta}=\sum_{pq}C_{\alpha p}C_{\beta q}(D^{\mathrm{eff}}_{qp}+D^{\mathrm{eff}}_{pq})\frac{\epsilon_p}{2}$$
$$+\sum_{Ip}C_{\alpha I}C_{\beta q}\sum_{rs}(D^F_{rs}+\bar{\kappa}_{rs})A_{rsIq}$$
$$+\frac{1}{2}\sum_{pq}C_{\alpha p}C_{\beta q}\sum_{x=a,b,c}\{H^x_{pq}+\Omega^a_{qp}\}, \tag{20}$$

$$\eta^{\kappa}_{AI}=\frac{1}{2}(D^F_{AI}+D^F_{IA})(\epsilon_I-\epsilon_A)-\frac{1}{4}\sum_{pq}(D^F_{pq}+D^F_{qp})A_{pqAI}$$
$$+\sum_{x=a,b,c}\{H^{(x)}_{AI}-\Omega^{(x)}_{AI}-H^{(x)}_{IA}+\Omega^{(x)}_{IA}\}. \tag{21}$$

The calculation of the RI-CC2 gradient can be sketched as follows:

(1) As in a conventional CC2 implementation, first the cluster amplitude equations are solved for t_μ and subsequently the Lagrangian multipliers $\bar{t}_\mu$ are determined. However, in the RI-CC2 approach only the single excitation parts t_{μ_1} and $\bar{t}_{\mu_1}$ are stored. To avoid storage bottlenecks, the double excitation parts are recalculated whenever needed from three-index integrals. From the solution of the cluster equations the intermediate Y^P_{ai} (see Table II) is available on file.

(2) Then all intermediates for the one- and two-particle densities which require the double excitation parts of either the cluster amplitudes or the Lagrangian multipliers are determined. This is done in two steps. First, the contraction $\Sigma_{ijc}\bar{t}^{ac}_{ij}t^{bc}_{ij}$ and the intermediates C_{ai}, $\bar{Y}^P_{ai}$, and $\check{Y}^P_{ai}$ are computed in a batched loop over the two involved occupied indices. Inside this $\bar{t}^{ab}_{ij}$ and t^{ab}_{ij} are calculated for a fixed pair i,j and contracted on-the-fly to the required intermediates. In the next step the contraction $\Sigma_{abk}\bar{t}^{ab}_{jk}t^{ab}_{ik}$ is evaluated in a similar loop but with occupied and virtual indices interchanged.

(3) After these n^5 scaling steps are completed, the three-index intermediates $\Gamma^{(x)}$ and the matrices $H^{(x)}$ with $x=a,b,c$ are evaluated from precalculated intermediates and different three-index integrals.

(4) From the intermediates $\Gamma^{(x)}$ the matrices $\Omega^{(x)}$ are calculated using the algorithm described in Ref. 10 for the closely related matrix $\Omega^{JG}_{\alpha i}$ used in the calculation of the residuum of the cluster equations.

(5) The one-particle density D^F and the inhomogeneity for the Z-vector equations η^{κ} are set up and the Z-vector

Downloaded 16 Apr 2003 to 141.52.232.84. Redistribution subject to AIP license or copyright, see http://ojps.aip.org/jcpo/jcpcr.jsp

equations are solved for the Lagrangian multipliers $\overline{\kappa}_{\mu_0}$. Then the effective one-particle density $D^{\mathrm{eff,ao}}$ and the effective Fock matrix $F^{\mathrm{eff,ao}}$ are calculated.

(6) After the densities and $F^{\mathrm{eff,ao}}$ are available, the derivative integrals are calculated and contracted on-the-fly to contributions to the gradient according to Eq. (11). For the four-center contribution $\Sigma_{\alpha\beta\gamma\delta} d^{\mathrm{sep,ao}}_{\alpha\beta\gamma\delta}(\alpha\beta|\gamma\delta)^{[x]}$ the separable two-particle density is only generated on-the-fly for fixed ao shell quadruples from $D^{\mathrm{eff,ao}}$ and $D^{\mathrm{scf,ao}}$. The three-center contribution $\Sigma_{P\alpha\beta}\Delta^{\mathrm{ao},P}_{\alpha\beta}(\alpha\beta|P)^{[x]}$ is evaluated in a batched loop over the ao index β. For each batch the density Δ^{ao} is calculated via Eq. (19) and then contracted with the integrals $(\alpha\beta|P)^{[x]}$.

III. THE ACCURACY OF CC2 FOR GROUND STATE EQUILIBRIUM STRUCTURES AND HARMONIC VIBRATIONAL FREQUENCIES

As pointed out in Sec. I, only little is known about the performance of the CC2 model for equilibrium geometries. Even though numerous CC2 calculations have been reported for excitation energies and a large variety of second- and higher-order properties, only few calculations[6,16,17] of equilibrium geometries have been reported. The results indicate that CC2 gives ground state geometries with a similar accuracy as obtained with MP2, but the investigated examples cover only a limited number of bonds.

To obtain a more systematic analysis of the accuracy of CC2 ground state equilibrium structures we employ a set[27] of 19 single-configuration dominated molecules recently introduced by Helgaker *et al.*[28] for a statistical analysis of equilibrium geometries of molecules consisting of hydrogen and first-row atoms for a number of standard single-reference methods and basis sets. For these molecules very accurate experimental and empirical results for the equilibrium geometries are available as reference.[29] From the original set used in Ref. 28 we had to leave out O_3, since for this case CC2 fails to converge. For the 19 molecules included, the MP2 and CC2 equilibrium structures (28 unique bond lengths and nine bond angles) have been determined for the correlation-consistent basis sets[30–33] cc-pVDZ, cc-pVTZ, and cc-pVQZ. These calculations have been carried out with the RI-MP2 program[14] of the TURBOMOLE package[34] and the RI-CC2 implementation described earlier. For the resolution of the identity the optimized auxiliary cc-pVDZ, cc-pVTZ, and cc-pVQZ basis sets from Ref. 35 were used. To determine the errors in the geometries introduced by the RI approximation, also conventional MP2 and CC2 calculations were carried using the programs MPGRAD[36] and DALTON.[8] For better comparison with Ref. 28 all electrons were correlated in these calculations.

The statistical analysis of the results for the 28 bond lengths is shown in Table IV. Essentially, for all three basis sets the MP2 and the CC2 methods yield very similar accuracies. In particular, if one compares the present results with, for example, the errors obtained at the CCSD(T)/cc-pVQZ level, which in Ref. 28 were determined as: $\overline{\Delta}=-0.12$ pm, $\overline{\Delta}_{\mathrm{abs}}=0.16$ pm, $\Delta_{\mathrm{std}}=0.20$ pm, and $\Delta_{\mathrm{max}}=0.61$ pm (for the set including O_3 and slightly different reference data). The most pronounced difference between the MP2 and the CC2 structures is an elongation of the bonds from MP2 to CC2 manifested in the ≈ 0.5 pm difference in mean errors $\overline{\Delta}$ obtained for all three basis sets. For the cc-pVDZ basis, which gives for most correlated methods considerably too long bonds, this leads to an increase of the mean absolute error $\overline{\Delta}_{\mathrm{abs}}$ by 0.5 pm from MP2 to CC2, but for the more accurate cc-pVTZ and cc-pVQZ basis sets very similar mean absolute errors are obtained for MP2 and CC2, since close to the basis set limit MP2 has a tendency to underestimate bond lengths, while CC2 has a tendency to give too long bond lengths. The standard deviations and the maximum errors are quite similar for all three basis sets and, as for MP2, the full accuracy of the CC2 method is first obtained with a triple-ζ basis, but no significant further improvement is obtained from a quadruple-ζ basis, since at this level the correlation error inherent to the second-order methods dominates. In this connection also the results for the segmented contracted TZVPP basis[37,38] are of interest. They are for MP2: $\overline{\Delta}=0.03$ pm, $\overline{\Delta}_{\mathrm{abs}}=0.50$ pm, $\Delta_{\mathrm{std}}=0.65$ pm, and $\Delta_{\mathrm{max}}=1.51$ pm. Thus, as seen from the results for the mean error ($\overline{\Delta}$), this basis gives geometries slightly less close to the basis set limit than obtained with cc-pVTZ, but due to a more favorable error cancellation at the MP2 level, the errors compared to experimental bond lengths are slightly smaller.

The above-mentioned results must be taken with some caution, since the details depend very much on the choice of the test set. Restricting the analysis to single bonds unveils that the difference between MP2 and CC2 depends on the bond type: for the cc-pVQZ basis one obtains in this case for

TABLE IV. Errors relative to experiment in calculated bond lengths R_e for MP2 and CC2 and relative RI errors in the bond lengths for RI-MP2 and RI-CC2. Listed are the mean errors $\overline{\Delta}=(1/n)\,\Sigma_{i=1}^{n}\Delta_i$, the mean absolute errors $\overline{\Delta}=(1/n)\,\Sigma_{i=1}^{n}|\Delta_i|$, the standard deviations $\Delta_{\mathrm{std}}=\sqrt{[1/(n-1)]\,\Sigma_{i=1}^{n}(\Delta_i-\overline{\Delta})^2}$, and the maximum absolute errors, $\Delta_{\mathrm{max}}=\max_i|\Delta_i|$ with $\Delta_i=R_e^X-R_e^{\mathrm{ref}}$. All errors are given in pm. For details concerning the test set and the reference values see the text. For the cc-pVQZ basis the CC2 results listed are obtained with the resolution-of-the-identity implementations, for the cc-pVDZ and the cc-pVTZ basis the results of conventional calculations are given.

		MP2		CC2	
Basis		Δ_{r_e}	Δ_{RI}	Δ_{r_e}	Δ_{RI}
cc-pVDZ	$\overline{\Delta}$	1.33	−0.0015	1.83	−0.0012
	$\overline{\Delta}_{\mathrm{abs}}$	1.33	0.0019	1.83	0.0019
	Δ_{std}	0.75	0.0018	0.94	0.0020
	Δ_{max}	3.16	0.0044	3.85	0.0048
cc-pVTZ	$\overline{\Delta}$	−0.13	−0.0001	0.33	−0.0002
	$\overline{\Delta}_{\mathrm{abs}}$	0.55	0.0007	0.63	0.0009
	Δ_{std}	0.67	0.0011	0.80	0.0013
	Δ_{max}	1.69	0.0034	1.97	0.0044
cc-pVQZ	$\overline{\Delta}$	−0.24	0.0001	0.30	
	$\overline{\Delta}_{\mathrm{abs}}$	0.51	0.0003	0.59	
	Δ_{std}	0.61	0.0004	0.74	
	Δ_{max}	1.74	0.0010	1.88	

Downloaded 16 Apr 2003 to 141.52.232.84. Redistribution subject to AIP license or copyright, see http://ojps.aip.org/jcpo/jcpcr.jsp

TABLE V. Bond lengths. Comparison of CC2 with MP2 and CCSD(T) results. All calculations were carried out using the cc-pVTZ basis and a frozen-core approximation ($1s$ for first-row and $1s2s2p$ for second-row atoms).

	MP2[a]			CC2			CCSD(T)[a]
Molecule	r_e	D_1	D_2	r_e	D_1	D_2	r_e
$\max(\lvert\Delta r_e^{MP2}\rvert,\lvert\Delta r_e^{CC2}\rvert)\leqslant 0.5$ pm							
HF	91.80	0.010	0.110	91.96	0.013	0.112	91.7
H_2O	95.91	0.009	0.116	96.05	0.013	0.118	95.9
NH_3	101.1	0.009	0.118	101.2	0.011	0.119	101.4
CH_4	108.5	0.010	0.116	108.6	0.012	0.116	108.9
HCl	127.3	0.007	0.124	127.4	0.011	0.125	127.7
BF	126.8	0.026	0.143	127.4	0.042	0.144	127.1
CH_2NH	102.0, 108.6,	0.026	0.166	102.1, 108.6	0.035	0.172	102.2, 108.8
	109.0, 127.5			109.1, 128.0			109.2, 127.7
C_2H_4	108.0, 133.2	0.024	0.163	108.1, 133.5	0.031	0.167	108.3, 133.7
0.5 pm$<\max(\lvert\Delta r_e^{MP2}\rvert,\lvert\Delta r_e^{CC2}\rvert)\leqslant$1 pm							
H_2	73.70	0.005	0.100	73.73	0.007	0.101	74.3
SiH_4	147.7	0.009	0.115	147.8	0.014	0.116	148.3
CH_2	110.4	0.009	0.127	110.5	0.013	0.128	111.0
H_2S	133.5	0.011	0.131	133.6	0.017	0.132	134.1
H_2O_2	96.44, 144.9	0.019	0.160	96.65, 146.4	0.025	0.168	96.40, 145.9
C_2H_2	106.2, 121.1	0.025	0.165	106.2, 121.6	0.032	0.170	106.4, 121.0
CH_2O	110.1, 121.0	0.035	0.162	110.2, 121.7	0.050	0.172	110.3, 121.0
Cl_2O	170.7	0.028	0.163	171.8	0.056	0.170	171.5
HNC	99.61, 117.6	0.029	0.152	99.75, 118.4	0.042	0.161	99.6, 117.5
N_2H_2	102.9, 125.6	0.028	0.175	103.0, 126.4	0.037	0.182	103.1, 125.4
1 pm$<\max(\lvert\Delta r_e^{MP2}\rvert,\lvert\Delta r_e^{CC2}\rvert)\leqslant$2 pm							
BCl	171.7	0.021	0.150	172.1	0.036	0.152	172.9
FOH	96.74, 142.4	0.028	0.166	96.98, 144.2	0.041	0.178	96.8, 143.8
ClOH	96.66, 169.7	0.019	0.155	96.89, 170.4	0.027	0.162	96.5, 170.9
CO_2	116.9	0.043	0.151	117.9	0.065	0.170	116.6
CO	113.8	0.036	0.146	114.9	0.054	0.158	113.6
HCN	106.4, 116.7	0.026	0.168	106.5, 117.4	0.034	0.175	106.7, 116.0
N_2	111.4	0.026	0.167	112.1	0.033	0.174	110.4
F_2	139.8	0.023	0.182	141.3	0.031	0.194	141.6
Cl_2	199.7	0.015	0.152	200.0	0.021	0.156	201.8
HNO	105.0, 122.1	0.036	0.180	105.4, 123.3	0.051	0.192	105.5, 121.4
2 pm$<\max(\lvert\Delta r_e^{MP2}\rvert,\lvert\Delta r_e^{CC2}\rvert)$							
P_2	192.6	0.028	0.194	194.0	0.039	0.204	191.6
C_2	126.0	0.051	0.264	128.0	0.092	0.302	125.1
C_3	130.0	0.050	0.196	131.2	0.077	0.218	130.2
CN^+	121.7	0.101	0.255	121.1	0.200	0.330	116.7
ClNO	113.7, 202.1	0.052	0.189	115.9, 203.1	0.111	0.217	114.1, 198.2
FNO	113.7, 153.3	0.052	0.172	115.1, 159.6	0.125	0.211	114.2, 149.7

[a]From Ref. 40, H_2 and H_2O_2 results from present work.

MP2 $\overline{\Delta}=-0.56$ pm, $\Delta_{std}=0.45$ pm, and $\Delta_{max}=1.74$ pm and for CC2 $\overline{\Delta}=-0.16$ pm, $\Delta_{std}=0.28$ pm, and $\Delta_{max}=0.62$ pm. If also the O–O, F–F, and F–O bonds, which are not described accurately at the MP2 level, are removed from the test set the results change to $\overline{\Delta}=-0.38$ pm, $\Delta_{std}=0.17$ pm, and $\Delta_{max}=0.70$ pm for MP2 and $\overline{\Delta}=-0.24$ pm, $\Delta_{std}=0.21$ pm, and $\Delta_{max}=0.62$ pm for CC2.

The test set employed for the above-mentioned study includes only nine bond angles. Therefore, a statistical analysis of the latter is abandoned. For all nine bond angles the CC2 results are rather close to the MP2 values, with a slightly larger tendency of CC2 to underestimate the experimental result, but this effect is rather minor.

In Table IV also an analysis of the RI errors in the equilibrium bond lengths are given. For the bond angles RI errors of 10^{-3}–10^{-2} deg are found. From these numbers it is obvious that the effect of the RI approximation on the equilibrium structures is negligible for all practical purposes, if auxiliary basis sets optimized as suggested in Refs. 35 and 37 are used. This corroborates again the results of a number of previous investigations,[10,13,35,37] which showed that the RI approximation does not lead to any significant loss of accuracy.

To study the difference in the trends of CC2 and MP2 equilibrium geometries in more detail and for a more representative set of molecules, we compare in Table V the bond lengths calculated for 34 molecules at the CC2/cc-pVTZ level with the respective MP2 results and the CCSD(T) val-

Downloaded 16 Apr 2003 to 141.52.232.84. Redistribution subject to AIP license or copyright, see http://ojps.aip.org/jcpo/jcpcr.jsp

ues as reference. These calculations were carried out with only the valence electrons correlated. To rationalize the results the recently suggested D_1 and D_2 diagnostics[39,40] are given in Table V, which are defined as

$$D_1 = \sqrt{\max\left(\lambda_{\max}\left[\sum_i t_{ai} t_{bi} \right], \lambda_{\max}\left[\sum_a t_{ai} t_{aj} \right] \right)}, \quad (22)$$

$$D_2 = \sqrt{\max\left(\lambda_{\max}\left[\sum_{ick} t_{ik}^{ac} t_{ik}^{bc} \right], \lambda_{\max}\left[\sum_{ack} t_{ik}^{ac} t_{jk}^{ac} \right] \right)}, \quad (23)$$

where $\lambda_{\max}[\mathbf{M}]$ is the largest eigenvalue of the matrix $\mathbf{M}$. The double-substitution amplitudes used for MP2 are those for the MP1 wave function, while the single-substitution amplitudes have to be taken from the MP2 wavefunction. For CC2 the single- and the double-substitution amplitudes are obtained as solution of the cluster equations.

For a better comparison, the molecules are sorted into four groups according to the maximum deviation between the MP2/CC2 and the CCSD(T) equilibrium bond lengths. The first group comprises mainly hydrides of first-row atoms and HCl and BF, only CH_2NH and C_2H_4 contain double bounds. For all these molecules the D_1 and D_2 diagnostics are small and there is little (0.1–0.2 pm) difference between the MP2 and CC2 bond lengths, with the exception of the C═N and C═C double bonds in CH_2NH and C_2H_4, respectively. For these two molecules the diagnostics are also somewhat larger than for the other molecules. The CC2 bond lengths are slightly larger than the corresponding MP2 values and, for these molecules, mostly somewhat closer to the CCSD(T) reference.

The second group, for which the MP2/CC2 results deviate at most by 1 pm from the CCSD(T) bond lengths, still contains mainly well-behaved closed-shell molecules, but also some intermediate cases with double and triple bonds. For the latter cases we observe the largest deviations between CC2 and CCSD(T): the double bonds in CH_2O (0.7 pm) and N_2H_2 (1.0 pm) and the triple bonds in C_2H_2 (0.6 pm) and HNC (0.9 pm). The respective MP2 bond lengths are still close to the CCSD(T) reference, deviating not more than 0.2 pm. But there is also one case—the electron-rich compound Cl_2O—where MP2 underestimates the bond length as much as 0.8 pm, while the CC2 result deviates not more than 0.3 pm from the CCSD(T) value.

The third group, where the MP2 and/or the CC2 bond lengths deviate more than 1 pm from the CCSD(T) values comprises the difficult cases with strong correlation effects, as clearly indicated by the D_1 and D_2 diagnostics. Let us we first consider the molecules with $D_2(\mathrm{CC2}) < 0.2$. The results for these cases underpin the trends found for the previous group of molecules: the relaxation of the single-substitution amplitudes in CC2 leads to an overestimation of the bond lengths for strong double or triple bonds, e.g., CO_2 (1.3 pm), CO (1.3 pm), HCN (1.4 pm), N_2 (1.7 pm), HNO (1.9 pm). But we also observe the improvement in bond lengths for single bonds between atoms with several lone pairs, as FOH, ClOH, and F_2, where the MP2 results are too short by 1.2–1.8 pm. For these molecules the $D_1(\mathrm{CC2})$ diagnostic is between 0.02 and 0.065 and $D_1(\mathrm{CC2})$ is between 0.15 and 0.2, indicating strong correlation effects. For the last six molecules in Table V with $D_2(\mathrm{CC2}) > 0.2$ the errors in the MP2 and the CC2 bond lengths become larger then 2 pm, which shows that second-order methods are inadequate to describe accurately the electronic structure of these molecules. This is in particular the case for the last three molecules where the D_1 diagnostics indicate also notable static correlation effects. It is, however, encouraging that strong correlation effects that may lead to problems in the CC2 bond lengths are reliably indicated by the D_1 and D_2 diagnostics.

In Table VI the harmonic frequencies obtained with the CC2 model are compared for a subset of the above-mentioned molecules with the MP2 results and CCSD(T) values as reference. Not unexpected, the accuracy obtained for the harmonic frequencies goes very much in parallel with that obtained for bond lengths, in particular for stretching modes. In almost all cases, the CC2 harmonic frequencies are below the respective MP2 values. For stretching modes corresponding to single and C═C double bonds the CC2 results are thereby somewhat closer to the CCSD(T) reference values than the MP2 harmonic frequencies. In most cases the differences between the CC2 and the MP2 results are only minor. Only for the stretching modes in some compounds with several lone pairs (F_2, Cl_2, Cl_2O, FOH) the CC2 model improves considerably upon MP2. However, for most double bonds and for all triple bonds CC2 gives harmonic frequencies for the stretching modes, which are too low by 60 cm^{-1} (C═O in CH_2O) to 250 cm^{-1} (N_2). On average CC2 gives harmonic frequencies of similar accuracy as obtained with MP2, deviating by about $30-50\ \mathrm{cm}-1$ from the CCSD(T) reference values, which are close to the experimental results.

IV. LARGE SCALE APPLICATIONS: THE EQUILIBRIUM GEOMETRIES OF *TRANS*-AZOBENZENE AND *CIS,TRANS*-1,4-DIFLUOROBUTADIENE

To test the implementation of the RI-CC2 ground state gradient in typical applications, the equilibrium geometry of *trans*-azobenzene and the geometry and harmonic frequencies of *cis,trans*-1,4-difluorobutadiene.

Let us first consider *trans*-azobenzene. This molecule and its derivatives play an important role in the development of materials for optical data storage.[41–44] The equilibrium structure of *trans*-azobenzene has for many years been subject of an ongoing discussion in the literature, since different experimental investigations came to contradictory conclusions about the symmetry of the ground state, i.e., whether it is planar with C_{2h} symmetry or distorted to C_2 or C_i symmetry. Only recently could it be shown that the gas-phase equilibrium geometry indeed has C_{2h} symmetry.[45,46] The mechanism exploited for optical data storage involves a *cis/trans* isomerization induced by excitation to the lowest $\pi \rightarrow \pi^\star$ excited states. The excited states of *trans*-azobenzene are therefore subject of intensive theoretical investigations.[11,46–48] As pointed out in Sec. I, in particular a study of adiabatic transitions relies on an accurate description also of the ground state by the methods employed for the excited states. In this context it is of interest to know whether the CC2 model gives an accurate ground state equilibrium structure for *trans*-azobenzene, and to which extent the CC2

Downloaded 16 Apr 2003 to 141.52.232.84. Redistribution subject to AIP license or copyright, see http://ojps.aip.org/jcpo/jcpcr.jsp

TABLE VI. Harmonic frequencies. Comparison of CC2 with MP2 and CCSD(T) results. All calculations were carried out using the cc-pVTZ basis and a frozen-core approximation ($1s$ for first-row and $1s2s2p$ for second-row atoms).

Molecule	MP2[a]	CC2	CCSD(T)[a]
$\max(\lvert\Delta r_e^{MP2}\rvert,\lvert\Delta r_e^{CC2}\rvert)\leqslant 0.5$ pm			
HF	4180	4149	4177
H_2O	1652,3855,3976	1649,3830,3951	1669,3841,3946
NH_3	1088,1687,3512, 3655,	1092,1684,3497, 3637	1109,1688,3472, 3598
CH_4	1350,1586,3076, 3212	1348,1584,3070, 3202	1344,1571,3035, 3154
HCl	3054	3046	3000
BF	1416	1391	1403
CH_2NH	1075,1101,1177, 1378,1494,1679, 3090,3197,3482	1068,1091,1169, 1370,1481,1653, 3078,3186,3466	1073,1081,1162, 1387,1483,1675, 3052,3152,3441
C_2H_4	828,960,983, 1076,1247,1384, 1485,1684,3179, 3197,3268,3294	825,948,977, 1072,1244,1376, 1481,1667,3174, 3190,3260,3287	823,942,967, 1047,1242,1369, 1479,1672,3139, 3157,3219,3246
$0.5\text{ pm}<\max(\lvert\Delta r_e^{MP2}\rvert,\lvert\Delta r_e^{CC2}\rvert)\leqslant 1$ pm			
H_2	4527	4521	4409
SiH_4	951,1004,2296, 2303	948,1002,2294, 2300	931,984,2251 2259
CH_2	1430,2990,3067	1428,2981,3055	1407,2912,2983
H_2S	1211,2780,2799	1209,2773,2791	1204,2717,2732
C_2H_2	589,753,1975, 3446,3541	563,743,1933, 3442,3531	578,747,2001, 3410,3511
CH_2O	1209,1280,1553, 1772,2970,3043	1197,1266,1533, 1723,2951,3013	1192,1275,1543, 1781,2929,2996
Cl_2O	301,657,740	289,634,699	294,644,700
HNC	503,2025,3837	470,1942,3810	473,2045,3825
N_2H_2	1347,1348,1513, 1622,3320,3354	1337,1338,1447, 1610,3303,3334	1328,1350,1558, 1622,3269,3301
$1\text{ pm}<\max(\lvert\Delta r_e^{MP2}\rvert,\lvert\Delta r_e^{CC2}\rvert)$			
BCl	858	854	838
FOH	996,1412,3798	920,1375,3761	925,1397,3780
ClOH	769,1278,3802	746,1264,3765	731,1280,3809
CO_2	656,1332,2426	629,1253,2334	660,1346,2396
CO	2121	1985	2154
HCN	719,2027,3476	706,1954,3457	716,2111,3444
N_2	2195	2093	2346
F_2	1017	957	920
Cl_2	577	569	546
HNO	1486,1586,3028	1378,1546,2956	1540,1597,2938
$\overline{\Delta}$	19	−4	
$\overline{\Delta}_{abs}$	31	34	
Δ_{std}	37	54	
Δ_{max}	151	253	
w/o problem cases[b]			
$\overline{\Delta}$	24	9	
$\overline{\Delta}_{abs}$	27	24	
Δ_{std}	26	30	
Δ_{max}	118	112	

[a]From Refs. 39 and 40. For the CCSD(T) harmonic frequencies for C_2H_2, CH_4, CO, CO_2, H_2, H_2O, HCN, HF, NH_3, N_2, CH_2O, and F_2 see also Ref. 53.

[b]Without problem cases, i.e., the following stretching modes ν(F–O) (in FOH), ν(Cl–O) (in ClOH), ν(F–F) (in F_2), ν(Cl–Cl) (in Cl_2), ν(C–O) (in CO_2, CO), ν(C–N) (in HCN, HNC), ν(N–N) (in N_2, N_2H_2), ν(N–O) (in HNO).

TABLE VII. The CC2 equilibrium structure (R_e) of *trans*-azobenzene in comparison with the MP2 structure and experimental (R_0) results.

	Ab initio calculations		Experiments	
Bond	MP2/cc-pVTZ[a]	CC2/cc-pVTZ	GED[b]	GED[c]
	Bond length (pm)			
$N_2{=}N_1$	126.8	127.5	126.8	126.0(8)
$C_3{-}N_1$	141.7	141.9	142.7	142.7(8)
$C_5{-}C_3$	140.0	140.2	139.6	140.5
$C_7{-}C_3$	139.7	139.8	139.6	140.1
$C_9{-}C_7$	139.1	139.3	139.6	139.6
$C_{11}{-}C_9$	139.3	139.4	139.6	139.7
$C_{13}{-}C_{11}$	139.8	140.0	139.6	140.2
$C_{13}{-}C_5$	138.8	138.9	139.6	139.3
$H_{15}{-}C_5$	108.0	108.0	108.8	110.2(7)
$H_{17}{-}C_7$	108.1	108.2	108.8	110.2(7)
$H_{19}{-}C_9$	108.1	108.2	108.8	110.2(7)
$H_{21}{-}C_{11}$	108.1	108.1	108.8	110.2(7)
$H_{23}{-}C_{13}$	108.2	108.2	108.8	110.2(7)
	Angles (deg)			
$C_3{-}N_1{=}N_2$	113.7	113.6	114.5	113.6(8)
$C_5{-}C_3{-}N_1$	124.6	124.5	123.0	124.7(9)
$C_7{-}C_3{-}N_1$	115.1	115.0		
$C_3{-}C_5{-}C_{13}$	119.3	119.2		
$C_3{-}C_7{-}C_9$	120.1	120.0		
$C_5{-}C_{13}{-}C_{11}$	120.5	120.5		
$C_5{-}C_3{-}C_7$	120.3	120.3		
$C_{13}{-}C_{11}{-}C_9$	120.0	120.0		
$C_{11}{-}C_9{-}C_7$	119.8	119.7		
$H_{15}{-}C_5{-}C_3$	119.1	119.1		
$H_{23}{-}C_{13}{-}C_5$	119.7	119.7		
$H_{21}{-}C_{11}{-}C_{13}$	119.9	119.9		
$H_{19}{-}C_9{-}C_{11}$	120.2	120.1		
$H_{17}{-}C_7{-}C_9$	121.6	121.6		

[a]Second-order Møller–Plesset perturbation theory, Ref. 11.

[b]Gas electron diffraction, Ref. 54.

[c]Gas electron diffraction, Ref. 45; in addition to values given also the difference ($\angle C^{(5)}$-$C^{(3)}$-$N^{(1)}$-$\angle C^{(7)}$-$C^{(3)}$-$N^{(1)}$)/2 was determined to be 5.0(9).

bond lengths and angles differ from the MP2 and the experimental values. In Table VII the results for the CC2/cc-pVTZ geometry of *trans*-azobenzene are listed in comparison with the respective MP2 and the experimental (GED) results. The CC2 and MP2 calculations[11] were carried out using a frozen-core approximation for the $1s$ orbitals of carbon and nitrogen. For the numbering of the atoms see Fig. 1. This comparison shows that the results from the previous section are transferable to larger molecules. Apart from the N═N double bond, all other bond lengths and angles agree very well with the experimental results, keeping in mind that the latter refer to the vibrational averaged (R_0) parameters. Little difference—only 0.1–0.2 pm in the bond lengths and 0.1 deg in the bond angles—is found between the CC2 and the MP2 equilibrium structure. Only for the N═N double bond the difference is larger, here one finds again the trend already observed in Sec. III, namely that the lengths of multiple bonds are overestimated by 0.5–1.5 pm.

The second example, *cis,trans*-1,4-difluorobutadiene, is one of the compounds studied recently within a series of experimental investigations on the structures and vibrational-spectra of fluorinated unsaturated hydrocarbons.[49–52] In Table VIII the MP2 and CC2 equilibrium structures calculated within the cc-pVQZ basis sets are listed. For these cal-

Downloaded 16 Apr 2003 to 141.52.232.84. Redistribution subject to AIP license or copyright, see http://ojps.aip.org/jcpo/jcpcr.jsp

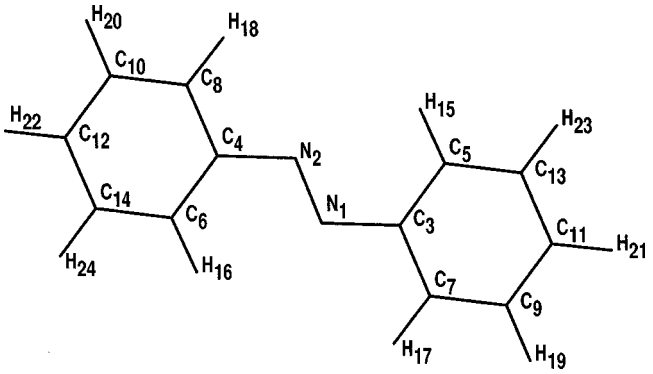


FIG. 1. *Trans*-azobenzene. Structure and enumeration of atoms.

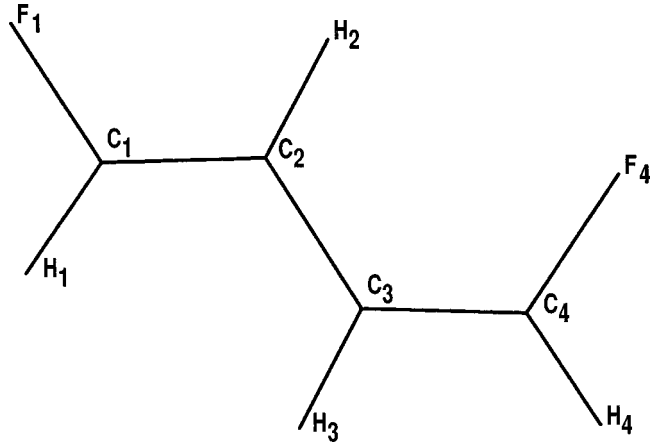


FIG. 2. *Cis, trans*-1,4-difluorobutadiene. Structure and enumeration of atoms.

culations again a frozen-core approximation was employed for the 1*s* orbitals of the carbon and fluorine atoms. For the numbering of the atoms see Fig. 2. The harmonic frequencies calculated with MP2 and CC2 in the cc-pVTZ basis (using geometries optimized with the same methods and basis sets) are listed in Table IX. Again, the comparison of MP2 and CC2 results for the bond lengths confirms the trends found in Sec. IV: while there is little difference in the bond lengths for the C_2-C_3 and C–H single bonds, the C═C double bonds and the C–F bonds are elongated by about 0.3 and 0.45 pm, respectively. Even though it is difficult to claim that either CC2 or MP2 is more appropriate for these molecules, from the findings of Sec. III one can expect that CC2 gives for this example the more accurate equilibrium structure. In particular, for the C–F and C═C bonds the MP2 results are expected to underestimate the true results for the equilibrium bond lengths (R_e). The experimental results of a very recent microwave study[52] listed for comparison in Table VIII are slightly closer to the structure obtained with CC2. This does, however, not really confirm the above-mentioned conclusion since the experimental results refer to the vibrational averaged structure (R_0), while the calculated results are equilibrium structures (R_e). In the present case, the experimental results—obtained by a fit to the microwave spectra of a number of isotopomers of $C_4H_4F_2$—are also affected by constraints imposed to the fit (the bond lengths and angles at the

TABLE VIII. The equilibrium structure of *cis,trans*-1,4-difluorobutadiene calculated at the CC2/cc-pVQZ level in comparison with the MP2 structure and the experimental result.

Bond/angle	MP2/cc-pVQZ	CC2/cc-pVQZ	Expt.[a] R_0
	Bond lengths (pm)		
C_2-C_3	144.5	144.5	143.9(18)
$C_1=C_2$	133.0	133.4	134.9(11)
$C_3=C_4$	133.1	133.4	134.5(2)
C_1-F_1	133.8	134.3	134.7(3)
C_4-F_4	134.2	134.7	134.7(3)
C_1-H_1	107.9	108.1	108.3(4)
C_2-H_2	107.9	108.1	108.2[b]
C_3-H_3	108.0	108.1	108.3[b]
C_4-H_4	107.7	107.8	109.2(2)
	Bond angles (deg)		
$C_1=C_2-C_3$	121.3	121.3	120.1(18)
$C_2-C_3=C_4$	124.2	124.2	123.1(8)
$C_2=C_1-H_1$	125.4	125.6	127.4(11)
$C_1=C_2-H_2$	119.2	119.3	119.0[b]
$C_4=C_3-H_3$	116.1	116.1	116.0[b]
$C_3=C_4-H_4$	125.4	125.6	126.4(3)
$C_2=C_1-F_1$	121.8	121.7	121.3(11)
$C_3=C_4-F_4$	121.7	121.7	121.2(2)
$H_1-C_1-F_1$	112.8	112.6	111.3(2)
$C_3-C_2-H_2$	119.6	119.5	120.9(7)
$C_2-C_3-H_3$	119.6	119.6	120.9(8)
$H_4-C_4-F_4$	112.9	112.8	112.3(1)

[a]From microwave spectroscopy, Ref. 52.
[b]Results of DFT calculations. For the fitting of the structure parameters to the results obtained from the microwave spectra the C_2-H_2 and C_3-H_3 bond lengths and the angles $C_1=C_2-H_2$ and $C_4=C_3-H_3$ were fixed to the results of a DFT calculations. Reference 52.

TABLE IX. Harmonic vibrational frequencies for *cis,trans*-1,4-difluorobutadiene calculated at the CC2/cc-pVTZ level in comparison with the MP2 harmonic frequencies and the experimental fundamental bands.

Band/symmetry		MP2/cc-pVTZ	CC2/cc-pVTZ	Infrared[a]	Raman[a]
ν_1	a'	3268	3258	3114	3114
ν_2	a'	3245	3235	3082	3078
ν_3	a'	3237	3229		3062
ν_4	a'	3228	3218		3036
ν_5	a'	1749	1725	1690	1679
ν_6	a'	1686	1658	1629	1621
ν_7	a'	1434	1421	1391	1385
ν_8	a'	1351	1341	1313	1313
ν_9	a'	1286	1272	1253	1252
ν_{10}	a'	1249	1239	1224	1219
ν_{11}	a'	1174	1168		1138
ν_{12}	a'	1168	1152	1129	1106
ν_{13}	a'	1033	1020	1017	1015
ν_{18}	a''	965	962	929	930
ν_{19}	a''	918	904	887	893
ν_{20}	a''	855	837	824	826
ν_{21}	a''	787	784	758	765
ν_{14}	a'	717	712	706	704
ν_{22}	a''	527	523		
ν_{15}	a'	512	506	504	505
ν_{16}	a'	305	302	308	312
ν_{23}	a''	242	246	230	242
ν_{24}	a''	162	157		155
ν_{17}	a'	136	136	138	146

[a]Infrared and Raman spectra from Ref. 52.

Downloaded 16 Apr 2003 to 141.52.232.84. Redistribution subject to AIP license or copyright, see http://ojps.aip.org/jcpo/jcpcr.jsp

atoms H_2 and H_3 were fixed to the results of a B3-LYP/TZ2P DFT calculation) and numerical problems, which lead to relatively large uncertainties for some structure parameters. The most evident difference between the experimental results and the *ab initio* calculated structures is that in the structure fitted to the microwave spectra the two C–F bonds have the same lengths, while the lengths for $C_1{=}C_2$ and $C_3{=}C_4$ bonds differ by 0.4 pm. On the contrary, the present MP2 and CC2 calculations and the B3-LYP/TZ2P density functional theory (DFT) calculations of Ref. 52 give in close agreement that there is little difference between the lengths of the two C=C double bonds and that the C_4-F_4 bond is about 0.4 pm longer than the C_1-F_1 bond. Another apparent difference is the C_2-C_3 bond length, which in MP2 and CC2 is obtained 0.6 pm shorter than the experimental value. The latter has, however, a rather large uncertainty (see Table VIII).

V. CONCLUSIONS

An analytic gradient of the second-order approximate coupled-cluster singles-and-doubles model CC2 has been implemented in the RI-CC2 program of the TURBOMOLE package. By virtue of the RI approximation the computational costs, i.e., CPU time, memory and disk space requirements are largely reduced compared to implementations employing conventional four-index electron repulsion integrals. Thereby, CC2 geometry optimizations for medium sized molecules with 10–30 atoms, which were challenging or impossible to carry out with previous implementations, become routine applications taking not more than a few hours or days of CPU time. As has been found before for MP2, the RI approximation leads also for CC2 only to negligible errors in equilibrium structures—far beyond experimental accuracies, if optimized auxiliary basis sets are used. With the recently suggested auxiliary basis sets for the correlation-consistent one-electron basis sets cc-pVXZ (X=D, T, Q), the RI errors in the bond lengths are of the order of 10^{-3} pm and the RI errors in the angles are about $10^{-3}-10^{-2}$ deg.

While structurally similar to MP2, differing only in the relaxation of the single-substitution amplitudes, CC2 shows notable differences in its trends for equilibrium geometries: multiple bonds, in particular triple bonds, are compared to MP2 elongated by 0.5–2 pm, which in many cases leads to an overestimation of the experimental values for R_e. On the contrary, for most single bonds, in particular for those between atoms with correlated lone pairs as, e.g., in Cl_2O and F_2, the CC2 bond lengths are somewhat closer to the CCSD(T) and the experimental values than the MP2 results. Overall, the present investigation, which covered 34 molecules with first- and second-row atoms and basis sets of different quality, shows that the CC2 model leads—as anticipated in previous publications—to equilibrium geometries of similar accuracy as obtained with MP2. The D_1 and D_2 diagnostics are found to be reliable indicators for static or strong dynamic correlation effects not adequately treated at the CC2 level. The accuracy obtained for harmonic frequencies goes in parallel with the trends observed for bond lengths. In most cases CC2 gives smaller harmonic frequencies than MP2. For stretching modes corresponding to single bonds the CC2 results are thereby mostly somewhat closer to the CCSD(T) and the experimental values, for most double bonds and, in particular, for triple bonds, where CC2 gives to long bond lengths, the harmonic frequencies for the corresponding stretching modes are considerably underestimated. The applicability of RI-CC2 geometry optimizations on molecules, which for conventional implementations are at present out of reach, has been demonstrated by calculations for the equilibrium structure of *trans*-azobenzene and *cis,trans*-1,4-difluorobutadiene. The CC2 equilibrium structure and harmonic frequencies for *cis,trans*-1,4-difluorobutadiene are the most accurate available *ab initio* results for this molecule.

Thus, the present results are quite encouraging for future applications of the RI-CC2 approach for the investigations of equilibrium structures and vibrational frequencies for excited states of medium sized molecules, which cannot be accessed by highly correlated methods as, for instance, CCSD or CC3 or multireference CI and coupled-pair functional methods. Work on this subject is in progress and will be reported in a forthcoming publication.[55]

ACKNOWLEDGMENTS

The author would like to thank a number of people who helped in accomplishing this work. He is grateful to Asger Halkier and Sonia Coriani for providing access to their notes about the CC2 gradient implementation in the DALTON program and he wishes to thank Andreas Köhn for valuable comments. Ida Beck Nielsen kindly made the MP2 and CCSD(T) harmonic frequencies from Refs. 39 and 40 available.

[1] T. Helgaker, P. Jørgensen, and J. Olsen, *Molecular Electronic-Structure Theory* (Wiley, New York, 2000).
[2] O. Christiansen, H. Koch, and P. Jørgensen, Chem. Phys. Lett. **243**, 409 (1995).
[3] R. J. Rico and M. Head-Gordon, Chem. Phys. Lett. **213**, 224 (1993).
[4] M. Head-Gordon, R. J. Rico, M. Oumi, and T. J. Lee, Chem. Phys. Lett. **219**, 21 (1994).
[5] R. Bauernschmitt and R. Ahlrichs, J. Chem. Phys. **104**, 9047 (1996).
[6] O. Christiansen, J. F. Stanton, and J. Gauss, J. Chem. Phys. **108**, 3987 (1998).
[7] A. Halkier, Ph.D. thesis, University of Aarhus, 1999.
[8] T. Helgaker, H. J. Å. Jensen, P. Jørgensen *et al.*, DALTON—an electronic structure program, release 1.2, 2001.
[9] K. Hald, A. Halkier, P. Jørgensen, C. Hättig, S. Coriani, and T. Helgaker, J. Chem. Phys. **118,** 2985 (2003).
[10] C. Hättig and F. Weigend, J. Chem. Phys. **113**, 5154 (2000).
[11] C. Hättig and K. Hald, Phys. Chem. Chem. Phys. **4**, 2111 (2002).
[12] C. Hättig, A. Köhn, and K. Hald, J. Chem. Phys. **116**, 5401 (2002).
[13] C. Hättig and A. Köhn, J. Chem. Phys. **117**, 6939 (2002).
[14] F. Weigend and M. Häser, Theor. Chem. Acc. **97**, 331 (1997).
[15] A. Köhn and C. Hättig, Chem. Phys. Lett. **358**, 350 (2002).
[16] O. Christiansen and P. Jørgensen, J. Am. Chem. Soc. **120**, 3423 (1998).
[17] O. Christiansen, J. Gauss, J. F. Stanton, and P. Jørgensen, J. Chem. Phys. **111**, 525 (1999).
[18] J. L. Whitten, J. Chem. Phys. **58**, 4496 (1973).
[19] B. I. Dunlap, J. W. D. Connolly, and J. R. Sabin, J. Chem. Phys. **71**, 3396 (1979).
[20] O. Vahtras, J. E. Almlöf, and M. W. Feyereisen, Chem. Phys. Lett. **213**, 514 (1993).
[21] M. W. Feyereisen, G. Fitzgerald, and A. Komornicki, Chem. Phys. Lett. **208**, 359 (1993).

Downloaded 16 Apr 2003 to 141.52.232.84. Redistribution subject to AIP license or copyright, see http://ojps.aip.org/jcpo/jcpcr.jsp

[22] T. Helgaker, P. Jørgensen, and N. C. Handy, Theor. Chim. Acta **76**, 227 (1989).
[23] P. J. Knowles, J. S. Andrews, R. D. Amos, and N. C. Handy, Chem. Phys. Lett. **186**, 130 (1991).
[24] D. J. Tozer, J. S. Andrews, R. D. Amos, and N. C. Handy, Chem. Phys. Lett. **199**, 229 (1992).
[25] T. J. Lee, S. C. Racine, J. E. Rice, and A. P. Rendell, Mol. Phys. **85**, 561 (1995).
[26] T. Helgaker and P. Jørgensen, Adv. Quantum Chem. **19**, 183 (1988).
[27] The test set consists of C_2H_2, C_2H_4, CH_2, CH_4, CH_2O, CO, CO_2, F_2, H_2, H_2O, H_2O_2, HCN, HF, HNC, HNO, HOF, N_2, N_2H_2, and NH_3.
[28] T. Helgaker, J. Gauss, P. Jørgensen, and J. Olsen, J. Chem. Phys. **106**, 6430 (1997).
[29] For all molecules except H_2O_2 we used as reference the empirical equilibrium bond lengths (R_e) and bond angles from F. Pawłowski, P. Jørgensen, J. Olsen, F. Hegelund, T. Helgaker, K. L. Bak, and J. F. Stanton, J. Chem. Phys. **116**, 6482 (2002). The equilibrium bond lengths (R_e) and bond angle for H_2O_2 were taken from G. Pelz, K. M. T. Yamada, and G. Winnewisser, J. Mol. Spectrosc. **159**, 507 (1993).
[30] T. H. Dunning, J. Chem. Phys. **90**, 1007 (1989).
[31] R. A. Kendall, T. H. Dunning, and R. J. Harrison, J. Chem. Phys. **96**, 6796 (1992).
[32] D. E. Woon and T. H. Dunning, J. Chem. Phys. **98**, 1358 (1993).
[33] D. E. Woon and T. H. Dunning, J. Chem. Phys. **100**, 2975 (1994).
[34] H. Weiss, R. Ahlrichs, and M. Haeser, J. Chem. Phys. **99**, 1262 (1993).
[35] F. Weigend, A. Köhn, and C. Hättig, J. Chem. Phys. **116**, 3175 (2002).
[36] F. Haase and R. Ahlrichs, J. Comput. Chem. **14**, 907 (1993).
[37] F. Weigend, M. Häser, H. Patzelt, and R. Ahlrichs, Chem. Phys. Lett. **294**, 143 (1998).
[38] A. Schäfer, C. Huber, and R. Ahlrichs, J. Chem. Phys. **100**, 5829 (1994).
[39] C. L. Janssen and I. M. B. Nielsen, Chem. Phys. Lett. **290**, 423 (1998).
[40] I. M. B. Nielsen and C. L. Janssen, Chem. Phys. Lett. **310**, 568 (1999).
[41] R. Hildebrandt, M. Hegelich, H.-M. Keller, G. Marowsky, S. Hvilsted, N. C. R. Holme, and P. S. Ramanujam, Phys. Rev. Lett. **81**, 5548 (1998).
[42] P. H. Rasmussen, P. S. Ramanujam, S. Hvilsted, and R. H. Berg, J. Am. Chem. Soc. **121**, 4738 (1999).
[43] S. J. Zilker, M. R. Huber, T. Bieringer, and D. Haarer, Appl. Phys. B: Lasers Opt. **68**, 893 (1999).
[44] Y. Sabi, M. Yamamoto, H. Watanabe, T. Bieringer, D. Haarer, R. Hagen, S. G. Kostromine, and H. Berneth, Jpn. J. Appl. Phys., Part 1 **40**, 1613 (2001).
[45] T. Tsuji, H. Takashima, H. Takeuchi, T. Egawa, and S. Konaka, J. Phys. Chem. A **105**, 9347 (2001).
[46] H. Fliegl, Diploma thesis, Universität Karlsruhe, 2002.
[47] P.-O. Åstrand, P. S. Ramanujam, S. Hvilsted, K. L. Bak, and S. P. A. Sauer, J. Am. Chem. Soc. **122**, 3482 (2000).
[48] P.-O. Åstrand, P. Sommer-Larsen, P. S. Ramanujam, S. Hvilsted, K. L. Bak, and S. P. A. Sauer, Chem. Phys. Lett. **325**, 115 (2000).
[49] N. C. Craig, C. F. Neese, T. N. Nguyen, C. M. Oertel, L. Pedraza, and A. M. Chaka, J. Phys. Chem. A **103**, 6726 (1999).
[50] B. Maté, A. Hight Walker, R. D. Suenram, and N. C. Craig, J. Phys. Chem. A **104**, 9489 (2000).
[51] N. C. Craig, C. M. Oertel, D. C. Oertel, and M. Lock, J. Phys. Chem. A **105**, 6008 (2001).
[52] N. C. Craig, C. M. Oertel, D. C. Oertel, M. J. Tubergen, R. J. Lavrich, and A. M. Chaka, J. Phys. Chem. A **106**, 4230 (2002).
[53] J. M. L. Martin, J. Chem. Phys. **100**, 8186 (1994).
[54] M. Traetteberg, I. Hilmo, and K. Hagen, J. Mol. Struct. **39**, 231 (1977).
[55] A. Köhn and C. Hättig (unpublished).

Downloaded 16 Apr 2003 to 141.52.232.84. Redistribution subject to AIP license or copyright, see http://ojps.aip.org/jcpo/jcpcr.jsp